Fuel 286 (2021) 119330

Contents lists available at ScienceDirect

Fuel

journal homepage: www.elsevier.com/locate/fuel

Full Length Article

Performance, emissions and end-gas autoignition characteristics of PREMIER combustion in a pilot fuel-ignited dual-fuel biogas engine with various CO_2 ratios

Alireza Valipour Berenjestanaki, Nobuyuki Kawahara *, Kazuya Tsuboi, Eiji Tomita

Graduate School of Natural Science and Technology, Okayama University, Tsushima-Naka 3-1-1, Kita-Ku, Okayama 700-8530, Japan

ARTICLE INFO

Keywords:
Autoignition
Biogas
Dual-fuel engine
PREMIER combustion
Thermal efficiency

ABSTRACT

Biogas, a renewable and alternative energy, has recently gained attention as an environmentally friendly fuel for power generation in internal combustion (IC) engines. This study aimed to investigate the effect of the carbon dioxide (CO_2) to methane (CH_4) ratio in a dual-fuel gas engine. It is known that gaseous fuel combustion at high loads is accompanied by knocking if an appropriate combustion controlling strategy is not applied. Therefore, premixed mixture ignition in the end-gas region (PREMIER) combustion was proposed under high load conditions. Experiments were carried out using a dual-fuel gas engine under supercharged conditions, with an intake pressure of 200 kPa. Simulated biogas consisting of CH_4 and CO_2 was used as a primary fuel and diesel was used as a pilot fuel. The pilot fuel injection timing was varied during the experiments. The indicated mean effective pressure (IMEP) and thermal efficiency increased as injection timing was advanced. With the addition of CO_2, the thermal efficiency of PREMIER combustion was slightly increased, although the IMEP was slightly decreased. The unburned gas temperature for PREMIER combustion increases as a function of the CO_2 content of the mixture. Due to compression by flame propagation, high unburned gas temperatures in dual-fuel gas engines are important for achieving autoignition inside the end-gas region under PREMIER combustion conditions.

1. Introduction

Excessive global emissions of carbon dioxide (CO_2) and other greenhouse gases (GHGs) from the burning of fossil fuels has led to a search for climate-friendly alternative fuels. Worldwide energy demand is increasing and consumption of fossil fuels, the current main source of energy, is increasing as a result. Depletion of petroleum resources is a concern, particularly for industries requiring internal combustion (IC) engines, which are widely used for transportation and power generation, among other industrial applications.

Biomass gas, which is considered to be a suitable renewable source of energy [1], is derived from animal, plant and food crop waste, as well as from human waste from sewage plants. This biological matter can be burned directly, or converted to liquid biofuels such as bioethanol and biodiesel, or gaseous biofuels that can be used as fuel for IC engines. Biogas is produced from biomass through decomposition of organic waste in an anaerobic environment. Biogas, which mainly consists of methane (CH_4) and CO_2, is flammable due to the high proportion of CH_4. Biogas contains 40–70% CH_4 and about 20–40% CO_2, along with small amounts of nitrogen and traces of oxygen and hydrogen sulfide [2]. The ratio of CH_4 and CO_2 in biogas varies depending on the generation method and raw materials used. Biogas is carbon–neutral, reduces landfill pollution, and is relatively cheap to produce. As an engine fuel, biogas has a relatively low laminar burning velocity and narrow flammability limits, which is important for engine performance. The energy density of biogas is relatively low due to the presence of CO_2. The lower heating value (LHV) of biogas is low but it has a high autoignition temperature; thus, biogas is resistant to knocking.

Biogas engines are used for electricity generation in both small- and large-scale plants [3,4]. In gas engines fueled with biogas, combustion can be initiated via a spark plug or diesel fuel. Biogas is widely used as a fuel in spark ignition (SI) engines [5–7]. Removal of CO_2 from biogas is often done to increase its heat value for use in spark-ignition engines, although the cost of the removal should be considered. Jingdang and Crookes studied the biogas fuel performance and exhaust emissions in an SI engine [5]. They reported that engine power and thermal efficiency were reduced when raw biogas of 60% CH_4 was used, compared to CO_2 removal conditions. The engine performance and thermal efficiency were improved by increasing the compression ratio, but nitrogen oxide

* Corresponding author.
E-mail address: kawahara@okayama-u.ac.jp (N. Kawahara).

https://doi.org/10.1016/j.fuel.2020.119330
Received 7 May 2020; Received in revised form 16 July 2020; Accepted 22 September 2020
Available online 20 October 2020

Nomenclature

ATDC	After top dead center
CH_4	Methane
CI	Compression ignition
CO	Carbon monoxide
CO_2	Carbon dioxide
$COV_{(IMEP)}$	Coefficient of variation of the indicated mean effective pressure
EGR	Exhaust gas recirculation
GHG	Greenhouse gas
HC	Hydrocarbon
HCCI	Homogeneous charge compression ignition
H_2O	Water
IC	Internal combustion
IMEP	Indicated mean effective pressure
KI	Knocking intensity
LHV	Lower heating value
NO_x	Nitrogen oxide
PI	PREMIER intensity
PLC	Programmable logic controller
PM	Particulate matter
PREMIER	Premixed mixture ignition in the end-gas region
RCCI	Reactivity controlled compression ignition
ROHR	Rate of heat release
SI	Spark ignition
θ_{ea}	End-gas autoignition
θ_{inj}	Injection timing of pilot fuel
τ	Ignition delay of initial combustion

(NO_x) and hydrocarbon (HC) emissions also increased [5]. Porpatham et al. investigated the effect of biogas CO_2 concentration (41%, 30% or 20% CO_2) in an SI engine: Increasing the ratio of CO_2 increased HC emissions but reduced CO and nitric oxide (NO) emissions, and engine performance [7].

The high autoignition temperature of biogas prevents its direct use in compression ignition (CI) engines; thus, an ignition source is needed. Dual fuel is considered the most suitable strategy for using biogas in CI engines. Dual-fuel engines typically use gaseous fuel (biogas) as the main fuel and liquid fuel (diesel) as a pilot fuel. In this type of combustion system, natural gas is often used; however, biogas is also used sometimes. The biogas fuel is introduced at the intake port and mixed with the inlet air. Due to the high autoignition temperature of biogas, combustion does not occur by solely compressing the biogas-air mixture. Therefore, liquid fuel (typically diesel fuel) is injected directly into the cylinder towards the end of the compression stroke as an ignition source. There are many studies on the application of biogas in CI engines operating in dual-fuel mode [8–19]. The effects of the equivalence ratio, biogas flow rate [2,9,10], compression ratio [11,12], biogas composition [8,13,14,15] and exhaust gas recirculation (EGR) [13] were investigated. In general, the biogas components that yield the best break thermal efficiency vary with engine speed and load, and the exhaust emissions of HC and CO increase compared to those of pure diesel engines [14]. Cacua et al. investigated biogas with 60% CH_4 and 40% CO_2 in a dual-fuel engine [16]. Oxygen-enriched air, from 21% to 27%, led to higher thermal efficiency and lower CH_4 emissions. Biogas engines using different pilot fuels, such as dimethyl ether (DME) [20] and biodiesel [17,18,21,22], have been studied. Yoon and Lee reported higher cylinder pressure and IMEP at high loads was obtained under biogas-biodiesel dual-fuel mode compared to single mode operation [18]. They also reported slightly lower thermal efficiency and NO_x emissions, and higher CO and HC emissions, under biogas-biodiesel dual-fuel mode compared to single mode operation. Advancing the injection timing increased the IMEP [20] and cylinder peak pressure [22].

Although gaseous fuels, including biogas, are suitable for dual-fuel operation, these fuels are limited due to knocking [23,24]. Biogas has been studied in homogeneous charged compression ignition (HCCI) [25–27] and reactivity controlled compression ignition (RCCI) mode [28]. In HCCI mode, knocking and misfiring occur when lower and higher amounts of biogas are used, respectively [26]. Knocking, which refers to unexpected end-gas autoignition accompanied by pressure oscillation, should be suppressed due to the potential for damage to engine components [29–31]. Dual-fuel operation under high load, high compression ratio and advanced injection timing conditions increases thermal efficiency [11,12], but may also increase the risk of knocking [19].

End-gas autoignition without pressure oscillation has been reported [32]; this can improve engine performance and thermal efficiency, and reduce emissions of CO and HC, which are typically higher under dual-fuel mode. This phenomenon has been named premixed mixture ignition in the end-gas region (PREMIER) combustion. PREMIER combustion differs significantly from normal combustion and knocking combustion in terms of its end-gas autoignition characteristics. Similar to the dual-fuel combustion system, pilot fuel autoignition triggers flame propagation of the gaseous fuel–air mixture, which releases combustion heat. The characteristics of unburned gas play an important role in determining the mode of combustion. If the propagating flame consumes the gaseous fuel–air mixture completely, normal combustion is achieved; otherwise, the unburned mixture will be auto-ignited in the end-gas region and will yield either knocking or PREMIER combustion. The histories of pressure and unburned gas temperature in the end-gas region are important determinants of the combustion mode, and can be controlled mainly by varying the injection timing of the pilot fuel. PREMIER combustion aims to improve the performance and thermal efficiency of IC engines [32–36]. Except for one study [35] demonstrating PREMIER combustion in an SI engine, our other studies were of dual-fuel gas engines operating under high load conditions. Azimov et al. showed that IMEP and thermal efficiency improved under PREMIER operation conditions when syngas of various compositions was used [33]. Split injection of pilot fuel was tested in terms of suppression of knocking to PREMIER combustion mode, and enhancement of normal to PREMIER combustion [34]. The strength of PREMIER combustion can be quantified in terms of PREMIER intensity (PI), as in the latest publication on this topic [36]. The previous works showed that engine performance and thermal efficiency can be improved, and emissions of CO and HC can be reduced (although those of NO_x slightly increase) with knock-free end-gas autoignition of an unburned mixture.

The purpose of this study is to investigate the effect of CO_2 on biogas engine performance parameters, such as the indicated mean effective pressure (IMEP) and thermal efficiency and exhaust emissions, at high load operation for stationary power generation engines. Under high load, the end gas autoignition characteristics are very important, particularly under PREMIER combustion conditions. A simulated gas consisting of CH_4 and CO_2 was used as the primary fuel, and a small amount of diesel was used as pilot fuel. The pilot fuel injection timing was varied during the experiments. Experiments were carried out using a dual-fuel engine under supercharged conditions with an intake pressure of 200 kPa while varying the ratio of CO_2 to CH_4. One of the goals of this study is to extend the PREMIER operation range by increasing the ratio of CO_2 to CH_4.

2. Experimental setup and data evaluation

The experiments were carried out using a single-cylinder, four-

stroke, water-cooled, direct-injection dual-fuel gas engine. The engine had a bore and stroke of 96 and 108 mm, respectively, with a displacement volume of 781 cm^3 and compression ratio of 15.9:1. A shallow-dish piston was used during the experiments. A solenoid-controlled injector with a three-hole nozzle (ϕ 0.11 mm) and a common rail system was used to spray the pilot fuel. The purpose of this nozzle was to inject as little diesel fuel as possible. The pilot fuel was delivered at an injection pressure of 40 MPa and rate of 1.6 mg/cycle, and the equivalence ratio was 0.015.

A schematic diagram of the experimental setup is shown in Fig. 1, and the engine details and experimental conditions are listed in Table 1. To detect the top dead center position of the camshaft, an optical sensor (photo interrupter) was used. The crank angle (CA) signal was detected with a photo-interrupter every 0.5°. The in-cylinder pressure was measured with a piezo-type pressure transducer (6052C; Kistler). A charge amplifier (5011; Kistler) was used to amplify the in-cylinder pressure signal. The gaseous fuel was introduced from the intake port and the gas flow rate was controlled with mass flow controllers. The gas flow rate was determined automatically using a programmable logic controller (PLC), to obtain accurate gas composition and equivalence ratio data. Simulated biogas consisting of CH_4 and CO_2 was used as the primary fuel, and diesel was used as the pilot fuel. The effect of the CO_2 to CH_4 ratio on engine performance, exhaust emissions and end-gas autoignition characteristics was investigated. All tests were conducted at an engine speed of 1,000 rpm, and an intake pressure of 200 kPa. The equivalence ratio of gaseous fuel and air was set to 0.56 to achieve lean-burn combustion. The ratio of diesel fuel to gaseous fuel in equivalence ratio was very small, at 2%. Pilot fuel injection timing was varied during the experiments, and was advanced until knocking occurred.

Fig. 2 shows the fuel supply strategies in all fueling cases and Table 2 shows the gas composition. In this study, CO_2 was added via the intake pipe. The ratio of CO_2 to CH_4 was varied from 0 to 50% by volume. The gaseous fuel flow rate is continuously adjusted based on the air flow rate readings obtained by the flowmeter, while the intake pressure was kept constant at 200 kPa. This strategy was applied to maintain a constant equivalence ratio throughout the experiments. As shown in Table 2, the

Table 1
Test engine specifications and experimental conditions.

Engine type Bore × stroke	Four stroke, single cylinder 96 mm × 108 mm
Displacement volume	781 cm^3
Equivalence ratio, ϕ_t	0.575
Compression ratio	15.9:1
Combustion system	Pilot ignited dual fuel combustion
Intake pressure, P_{in}	200 kPa
Injection system	Common rail direct injection
Injection pressure	40 MPa
Injection quantity	1.6 mg/cycle
Nozzle hole × diameter	3 hole × ϕ 0.11 mm
Engine speed	1000 rpm
Gaseous fuel supply	Premixed charged through intake port
Air intake	Supercharged condition
Intake valve open/close	340°ATDC/135°BTDC
Exhaust valve open/close	130°ATDC/345°BTDC

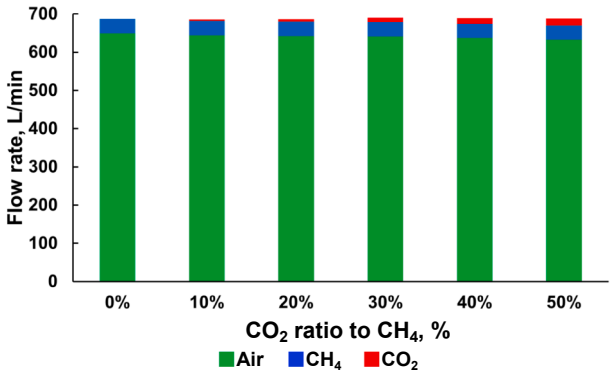

Fig. 2. Gaseous fuel supply strategy.

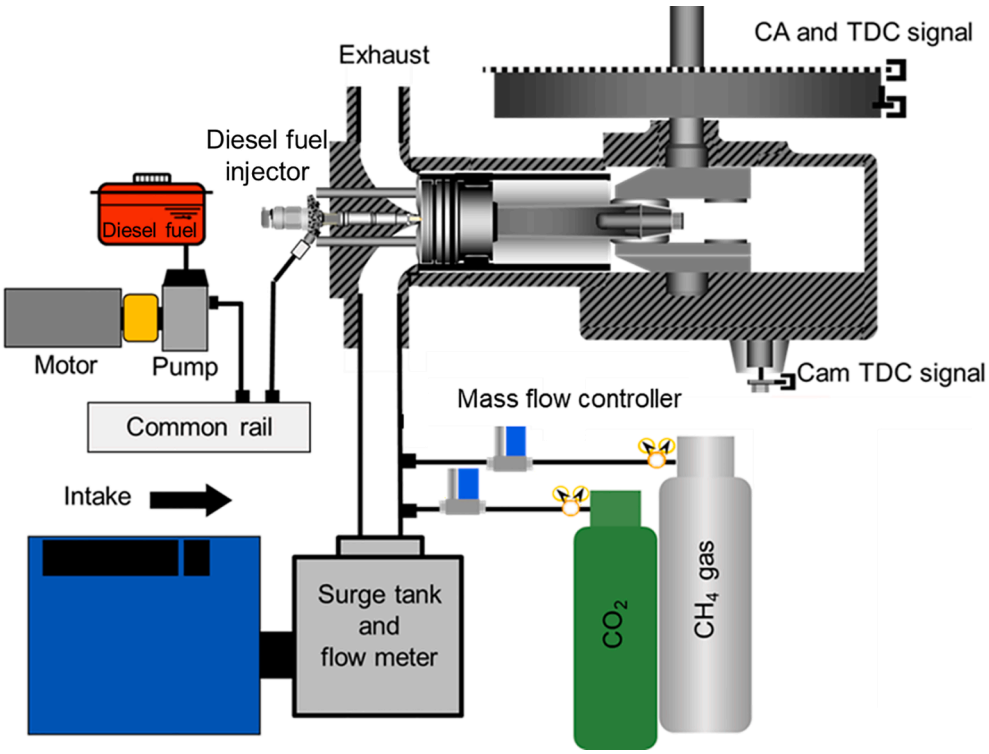

Fig. 1. Schematic diagram of the experimental setup.

Table 2
Gas composition.

CH_4	CO_2	Mass %			Heat value
(Vol.%)	(Vol.%)	Air	CH_4	CO_2	(J/cycle)
100	0	96.85	3.14	0	2788.8
100	10	96.03	3.11	0.85	2761.9
100	20	95.33	3.09	1.57	2758.9
100	30	94.41	3.06	2.51	2756.5
100	40	93.61	3.03	3.34	2736.6
100	50	92.83	3.01	4.15	2720.1

heat value was varied from 2,788.8 to 2,720.1 J/cycle, by changing the ratio of CO_2 to CH_4 from 0 to 50%.

To explore the main indicator of knocking, i.e., pressure oscillation, a band-pass-filter (4–20 kHz) was applied to all pressure history data. A knocking intensity (KI) $>$ 0.1 MPa was considered to indicate the occurrence of a knocking cycle; this threshold was selected based on the noise level of the pressure signal. Any cycles below the threshold were considered knock-free cycles of normal or PREMIER combustion [32]. The KI was used to distinguish normal, PREMIER and knocking combustion. A detailed explanation can be found in a previous publication [36].

In PREMIER combustion, it is important to know the unburned gas temperature inside the cylinder. After autoignition of diesel fuel, the propagating flame of the homogeneous mixture of CH_4 and CO_2 can be seen. The temperature and pressure of the end-gas region increases due to compression by the propagating flame. The unburned gas temperature in the cylinder was calculated based on the pressure history and volume of the cylinder, assuming a polytropic change in the cylinder between the time when the intake valve was closed and the time of diesel fuel injection, and assuming an adiabatic change after diesel fuel injection. The gas temperature was estimated under the assumption that the unburned gas is compressed by the propagating flame. Fig. 3 shows the gas temperature obtained based on the pressure history, under the injection timing condition of -13° after top dead center (ATDC) with no CO_2 addition. The polytropic index of the homogeneous mixture of CH_4 and CO_2 was estimated based on the pressure history and volume of the cylinder. Regarding the assumption of adiabatic change, the ratio of specific heats of the unburned gas mixture of CH_4 and CO_2 was determined with consideration of temperature dependence.

3. Results and discussion

As an example of the effect of the injection timing of pilot fuel, pressure history and rate of heat release (ROHR) data for the 20% CO_2 fueling case are shown in Fig. 4. The maximum in-cylinder pressure increased when injection timing was advanced. The maximum in-cylinder pressure occurs slightly earlier when the combustion phase is

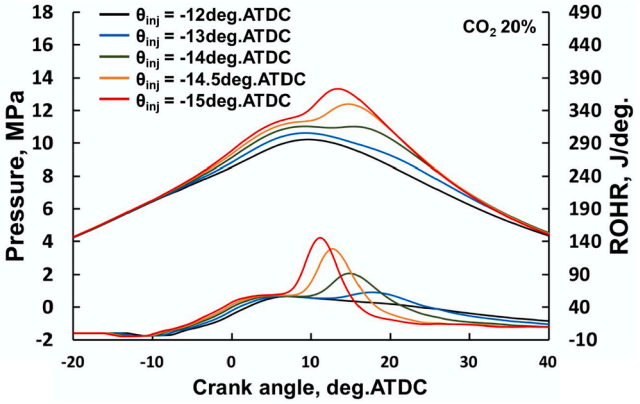

Fig. 4. Pressure history and rate of heat release with the 20% CO_2 mixture.

advanced. When the injection timing was advanced from injection timing (θ_{inj}) = -12° ATDC to -15° ATDC, the in-cylinder pressure at the time of pilot fuel injection decreased from 6.0 to 5.4 MPa. Three peaks in ROHR occur in dual fuel engines under the PREMIER and knocking combustion conditions. The first ROHR peak corresponds to pilot fuel autoignition. This is not always seen clearly. The second peak, which gradually increases and occurs close to TDC, corresponds to gaseous fuel–air combustion due to flame propagation. This is not always seen clearly because end-gas autoignition can occur early. The third peak corresponds to end-gas autoignition of the unburned mixture. In the experimental conditions shown in Fig. 4, the first peak in ROHR was not seen clearly due to the short ignition delay of the pilot fuel. After the main combustion period for the gaseous fuel–air mixture, the third peak can be seen at a CA of around 10–15° ATDC under PREMIER and knocking combustion conditions. In Fig. 4, the $\theta_{inj} = -13^\circ$ ATDC, $\theta_{inj} = -14^\circ$ ATDC and $\theta_{inj} = 14.5^\circ$ ATDC conditions show a third ROHR peak, which increases when injection timing is further advanced. Under these pilot injection timings, PREMIER combustion can occur. When the CA of the injection timing is advanced from -15° ATDC, there are some high-frequency components in the in-cylinder pressure that begin to shift toward knocking. By advancing the pilot fuel injection timing, combustion shifts from normal combustion due to flame propagation of the homogeneous mixture to PREMIER combustion with a third heat release peak in the end gas region due to compression by flame propagation.

Fig. 5 shows the pressure history and ROHR characteristics under the pure CH_4 and 10, 20, 30, 40 and 50% CO_2 conditions, under the optimal injection timing without knocking. The maximum in-cylinder pressure was observed under the 50% CO_2 condition, close to TDC. The minimum in-cylinder pressure was observed under the 10% CO_2 and pure CH_4 conditions. Generally, increasing the ratio of CO_2 to CH_4 tends to reduce

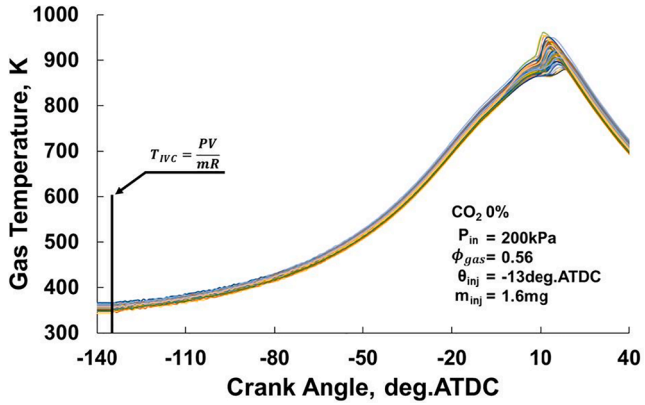

Fig. 3. Estimation of gas temperature from in-cylinder pressure.

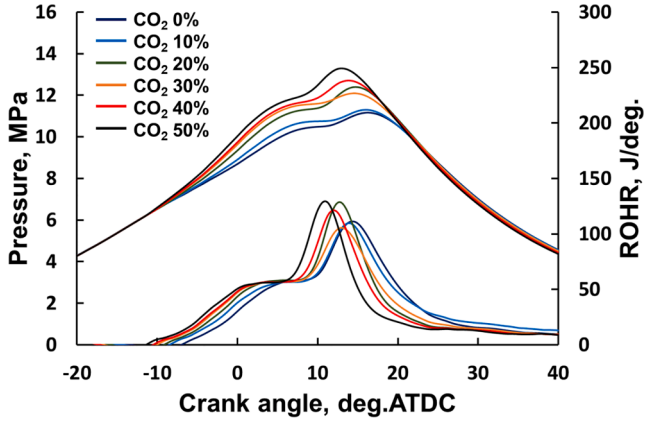

Fig. 5. Pressure history and rate of heat release of all fueling cases.

the peak pressure when the injection timing is not changed [8,15,20], whereas advancing the injection timing leads to a higher in-cylinder peak pressure, as shown in Fig. 4. The addition of CO_2 to CH_4 could make it possible to advance the pilot fuel injection timing over a wider range. Regarding the ROHR characteristics shown in Fig. 5, the first peak, caused by pilot fuel autoignition, could not be seen clearly; in particular, the ratio of CO_2 to CH_4 was lower. The second ROHR peak, during flame propagation, reached almost the same value.

Fig. 6 shows normal, PREMIER and knocking combustion (green, blue and red colors, respectively) at the time of pilot fuel injection with various CO_2 ratios. PREMIER combustion required PREMIER cycles to account for more than 50% of all cycles [36]. As the ratio of CO_2 to CH_4 increased, PREMIER combustion occurred under advanced pilot fuel injection timing conditions. The duration of pilot fuel injection timing for PREMIER combustion was almost the same, even under higher CO_2 to CH_4 ratios. Fig. 7 shows the percentage of normal, PREMIER and knocking combustion cycles. In the pure CH_4 case, all cycles showed PREMIER combustion at $\theta_{inj} = -12.5^\circ$ ATDC, although knocking occurred more than 20% of the time at $\theta_{inj} = -13.0^\circ$ ATDC. However, with CO_2 addition, when PREMIER combustion changed to knocking due to advanced timing of the CA (0.5°), the percentage of knocking was below 10%. Knocking appeared in only one cycle when the proportion of CO_2 in the CO_2 to CH_4 ratio was 10, 30 or 40%. In general, it is easy to control PREMIER combustion when the proportion of CO_2 is higher.

Fig. 8(a)–(c) show the IMEP, thermal efficiency, and coefficient of variation of the IMEP [$COV_{(IMEP)}$], respectively, as a function of the injection timing of the CO_2–CH_4 mixture. When injection timing was advanced and PREMIER combustion was achieved, IMEP increased, except in the 50% CO_2 condition. When injection timing is advanced, combustion is triggered earlier; therefore, a larger amount of heat is released in the advanced CA, leading to higher in-cylinder pressure and IMEP. As a result of end-gas autoignition, the maximum IMEP was obtained during PREMIER and knocking combustion under all fueling conditions. The IMEP under PREMIER combustion decreased slightly with CO_2 addition. Thermal efficiency was increased by advancing the injection timing for all CO_2–CH_4 mixtures. The maximum thermal efficiency was obtained under PREMIER combustion. Other researchers have reported a reduction in thermal efficiency with an increase in the CO_2 ratio [2,15,18]. However, in our experiment, the maximum thermal efficiency under PREMIER combustion was almost the same or slightly larger with an increase in the CO_2 ratio, although the increase in proportion of CO_2 in the mixture results in the heat decreasing slightly. Engine stability is indicated by $COV_{(IMEP)}$. When injection timing was advanced, $COV_{(IMEP)}$ was reduced under all fueling conditions. Stability was improved under PREMIER combustion, regardless of the CO_2 fraction in the mixture. The $COV_{(IMEP)}$ of the PREMIER operation mode for all fueling conditions is less than 5%.

Exhaust emissions of NO_x, THC and CO are shown in Fig. 9(a)–(c), respectively. In this study, advancement of injection timing promoted NO_x emissions. It has been reported that with a fixed overall equivalence

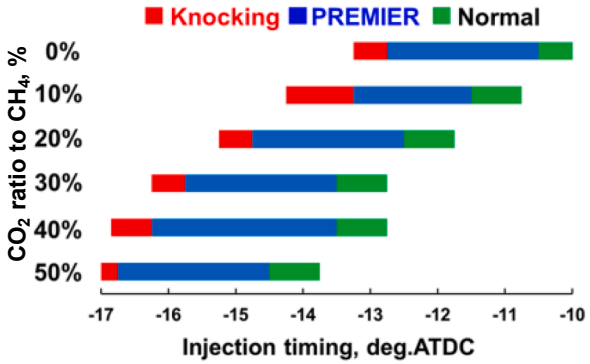

Fig. 6. Operating range of normal, PREMIER and knocking.

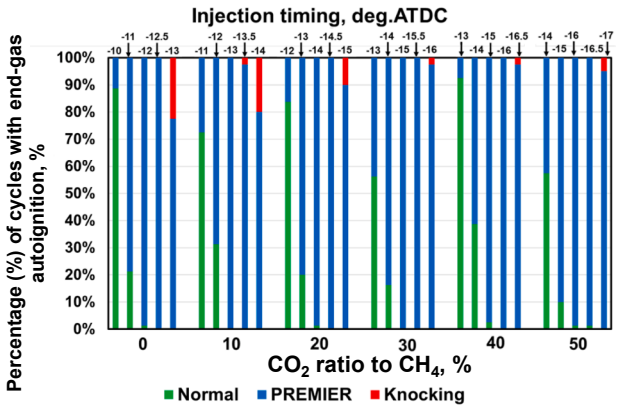

Fig. 7. End-gas autoignition (%).

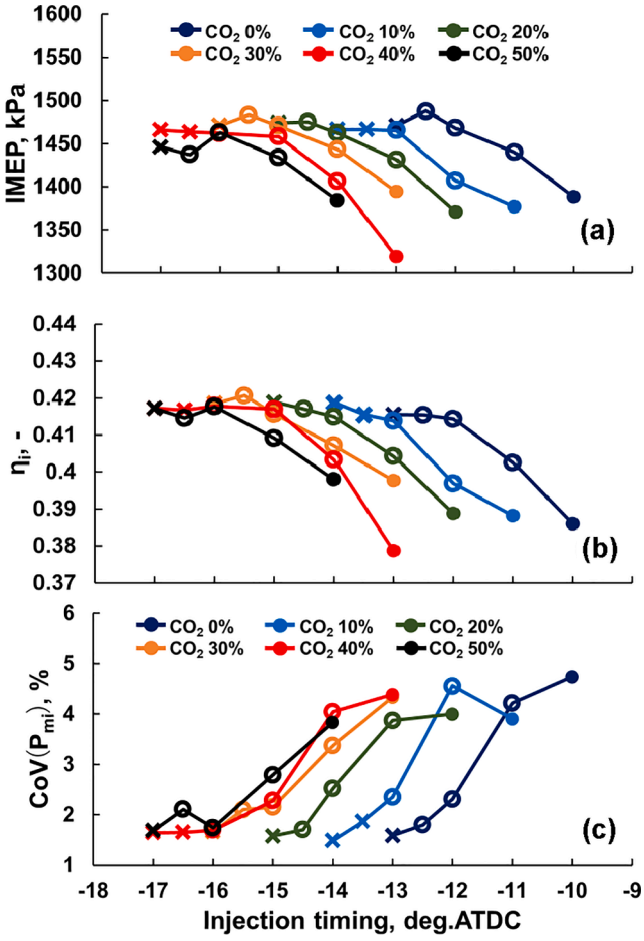

Fig. 8. Engine performance: (a) indicated mean effective pressure (IMEP); (b) indicated thermal efficiency; (c) coefficient of variation of the IMEP.

ratio, advancing injection timing increases NO_x emissions [19]. When injection timing is advanced, ignition is triggered at an earlier stage; thus, more fuel burns, causing higher peak cylinder temperatures and, consequently, more NO_x emissions. In this study, NO_x emissions were highest under knocking combustion, followed by PREMIER combustion. This result may be due to the higher cylinder temperatures resulting from advanced combustion (in turn due to end-gas autoignition). NO_x emissions during PREMIER combustion slightly decreased with a higher proportion of CO_2 in the CO_2–CH_4 mixture, due to the presence of non-reactive CO_2 (which lowers the combustion temperature). It is known

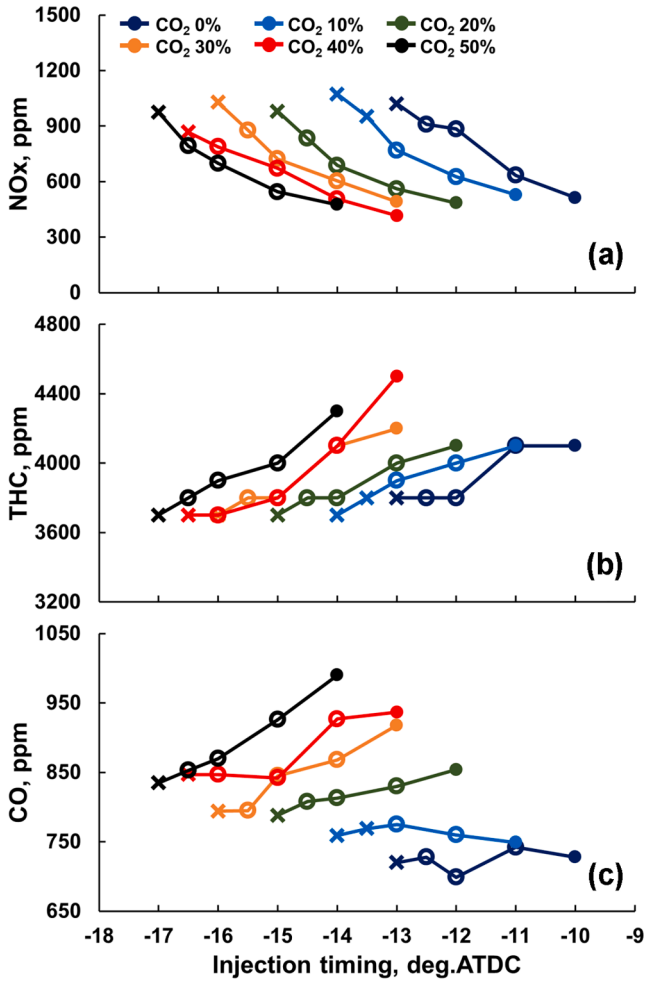

Fig. 9. Exhaust emissions of: (a) NO_x; (b) unburned hydrocarbon (THC); (c) carbon monoxide (CO).

that NO_x emissions are highly temperature-dependent, so by increasing the proportion of CO_2 in the mixture, less NO_x is emitted [18]. In this study, a slight decrease in heat under larger CO_2 to CH_4 ratios also reduced NO_x.

Both THC and CO increase with a higher proportion of CO_2 in the CO_2–CH_4 mixture, due to the lower combustion temperature [18,19]. The minimum THC and CO emissions were observed under PREMIER combustion with advanced injection timing, due to end-gas autoignition. Under PREMIER operation mode, the unburned mixture undergoes autoignition after the main combustion period for the gaseous fuel–air mixture; therefore, the THC and CO emissions decrease. THC emissions under PREMIER combustion were almost the same among all fueling cases. As shown in Fig. 9(c), CO emissions under PREMIER combustion slightly increased with increases in the CO_2 to CH_4 ratio.

In a previous study, particulate matter (PM) was measured with an opacimeter using natural gas, and the amount was found to be negligible even though the experimental conditions were similar (albeit not identical) [32]. Furthermore, the ratio of 50% CO_2 to CH_4, corresponds to only 2.7% of the volume of the total gas, as shown in Fig. 2. The equivalence ratio of diesel fuel is 0.015, while the equivalence ratio of gaseous fuel with CH_4 is 0.56. The ratio of diesel fuel to gaseous fuel is only 2%. Hence, the PM amount was considered to be almost zero due to the small amount of diesel fuel and addition of CO_2 in this work.

Fig. 10 shows the ROHR and mass fraction burned (MFB) at $\theta_{inj} = -13°$ ATDC for pure CH_4 and mixtures with 10, 20, 30, 40 and 50% CO_2. Heat generation was slightly reduced by the addition of CO_2, due to the effect of slow combustion (with CO_2 acting as an inert gas). During the

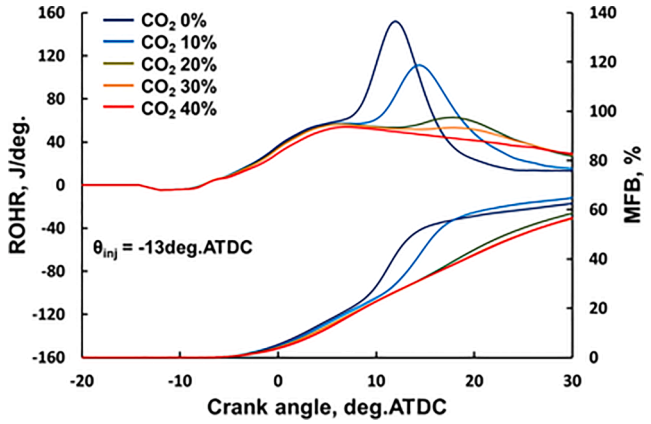

Fig. 10. The rate of heat release (ROHR) and mass fraction burned (MFB) with $\theta_{inj} = -13°$ ATDC for all fueling cases.

initial combustion period, often considered to correspond to 0 to 5% of the MFB, heat generation is increased due to autoignition of the pilot fuel. The period from 5 to 20% of the MFB corresponds to the main flame propagation period of combustion of the homogenous CH_4, air and CO_2 mixture. After this combustion period, end-gas autoignition occurs due to the increase in pressure and temperature of the unburned gas compressed by propagating flame, as well as the flame propagation.

Fig. 11 shows the ignition delay as a function of θ_{inj}, with different ratios of CO_2 to CH_4. Ignition delay is the time difference between the start of injection and initiation of ignition. Increasing CO_2 or advancing injection timing resulted in a longer ignition delay. When pilot fuel injection timing is advanced, the in-cylinder mixture temperature and pressure are lower at the point of fuel injection; therefore, autoignition takes longer, resulting in a longer ignition delay. The ignition delay increased when the ratio of CO_2 to CH_4 increased, owing to a lower ratios of specific heats. Mixtures with a lower ratio of specific heat have a lower unburned gas temperature; thus, it takes longer for the mixture to be auto-ignited. Similar results were reported by other studies [2,8,18,20].

Fig. 12 shows the pressure history, ROHR, unburned gas temperature estimated from the in-cylinder pressure and volume, and MFB with 20% CO_2. The pressure and ROHR shown in Fig. 4 are presented again in the upper part of Fig. 12 to show the relationship between these factors clearly. As the pilot fuel injection was advanced, the ignition delay of the diesel fuel became slightly longer, as shown in Fig. 11. However, the effect of advanced CA of injection timing is larger, leading to advanced combustion and increased pressure and temperature. The initial combustion period (from 0% to 5% of the MFB) is strongly affected by the ignition delay and autoignition of the pilot fuel. During this combustion period (from 5% to 20% of the MFB), premixed flame propagates, and a second peak appears before autoignition inside the end-gas region. The unburned gas temperature of the end-gas region at the time of heat

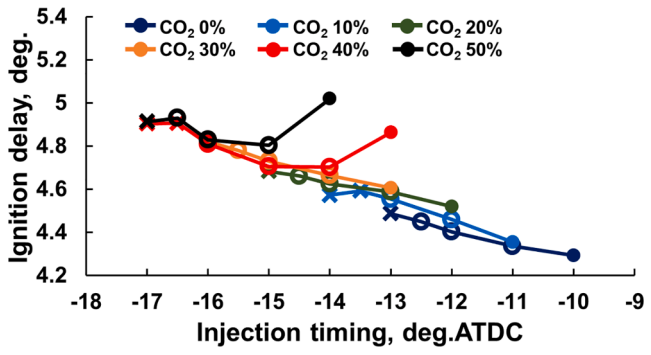

Fig. 11. Ignition delays during initial combustion.

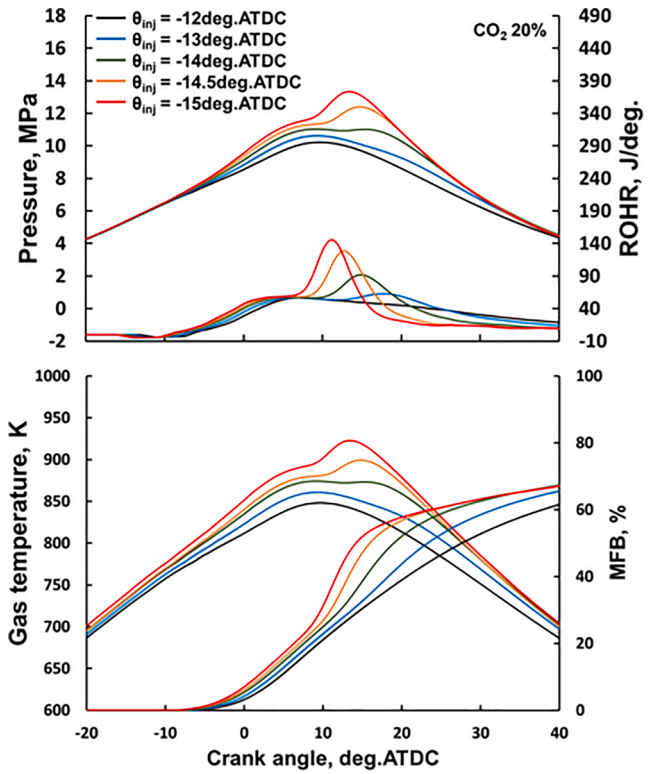

Fig. 12. Pressure, ROHR, unburned gas temperature and mass fraction burned (MFB) with the 20% CO_2 mixture (Pressure and ROHR are the same as in Fig. 4.).

generation during PREMIER or knocking combustion increased as the timing of the pilot fuel injection was advanced. The end-gas region, which is compressed by flame propagation, is supposed to be adiabatically compressed; flame propagation of the main fuel raises the unburned gas temperature, resulting in autoignition inside the end-gas region. In this study, we investigated the effect of CO_2 content on autoignition characteristics inside the end-gas region.

Fig. 13 shows the in-cylinder pressure at the initiation of end-gas autoignition (θ_{ea}) as a function of the proportion of CO_2 in the CO_2–CH_4 mixture; each value represents the average of 80 cycles. Filled circles, unfilled circles and crosses indicate normal, PREMIER and knocking combustion, respectively. The dashed line in Fig. 13 shows that in-cylinder pressure increases with the proportion of CO_2 in the mixture. The cylinder pressure at θ_{ea} for PREMIER combustion was 10.6 MPa for the 0 and 10% CO_2 mixtures, 11.2–11.4 MPa for the 20 and 40% CO_2 mixtures, and 11.6 MPa for the 50% CO_2 mixture. Above these

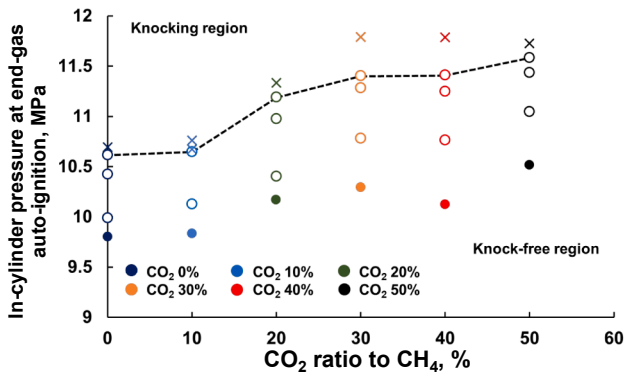

Fig. 13. In-cylinder pressure at the initiation timing of end-gas autoignition by the CO_2– CH_4 ratio.

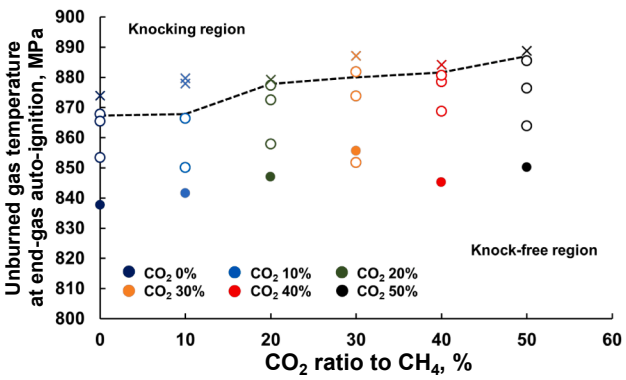

Fig. 14. Unburned gas temperature at the initiation timing of end-gas autoignition by the CO_2– CH_4 ratio.

pressure levels, knocking was observed. Fig. 14 shows the unburned gas temperature at θ_{ea} in the cases of PREMIER and knocking combustion. The dashed line in Fig. 14 shows the unburned gas temperature at θ_{ea} for each CO_2 ratio. The addition of CO_2 increased the unburned gas temperature at θ_{ea} without knocking. The pressure and temperature at the time of autoignition inside the end-gas region increased as the amount of CO_2 increased. This result is due to a reduction in the ratio of specific heats and a reduction of the flame propagation speed. Knocking was suppressed even when the injection timing of the pilot fuel was advanced. When CO_2 was mixed into the main fuel, PREMIER combustion was achieved by advancing the injection timing of diesel fuel at an appropriate CA. When the CO_2 ratio is high, even if the temperature of the end gas is also high, the inert gas CO_2 helps prevent knocking; thus, PREMIER combustion can be achieved.

The effect of CO_2 on ignition delay is very interesting because the role of CO_2 is usually discussed from the perspective of biogas and EGR, which contains CO_2 and H_2O. This effect is considered to be thermal and/or chemical. Based on simulations of chemical reactions, Tingas et al. reported that the addition of CO_2 affects the adiabatic and isochoric autoignition of CH_4-air mixtures in an entirely thermal manner, and further that the ignition delay becomes longer upon the addition of 15% CO_2 at a pressure of 3 MPa and equivalence ratio of 0.8 [37]. Although the conditions in this study differ from those in Ref. [37], the effect of the addition of CO_2 is only considered as a thermal effect with larger heat capacity, which leads to the lower unburned gas temperature. The effect of CO_2 on ignition delay will be discussed in detail in future studies using simulations of chemical reactions.

4. Conclusion

In this study, experiments were carried out on a dual-fuel gas engine at a constant speed of 1,000 rpm, with different pilot fuel injection timings under supercharged conditions and with an intake pressure of 200 kPa. Simulated biogas containing CH_4 and CO_2 was used. The additional ratio of CO_2 to CH_4 was varied from 0 to 50%. Engine performance, emissions and end-gas autoignition characteristics were evaluated. The following results were obtained:

1. PREMIER combustion was observed even when the volume ratio of CO_2 to CH_4 was increased. The maximum in-cylinder pressure under optimal pilot fuel injection timing increased with increasing CO_2 content. The addition of CO_2 suppressed knocking such that more knock-free end-gas autoignition cycles were achieved.
2. IMEP and thermal efficiency increased when injection timing was advanced. With the addition of CO_2, the thermal efficiency of PREMIER combustion was slightly increased, although the IMEP was slightly decreased.

3. The unburned gas temperature for PREMIER combustion increases as a function of the CO_2 content of the mixture. Due to compression by flame propagation, high unburned gas temperatures in dual-fuel gas engines are important for achieving autoignition inside the end-gas region under PREMIER combustion conditions.

CRediT authorship contribution statement

Alireza Valipour Berenjestanaki: Investigation. **Nobuyuki Kawahara:** Conceptualization, Methodology, Validation, Investigation, Writing - original draft. **Kazuya Tsuboi:** Resources. **Eiji Tomita:** Conceptualization, Validation, Writing - review & editing, Funding acquisition, Supervision.

Declaration of Competing Interest

The authors declare that they have no known competing financial interests or personal relationships that could have appeared to influence the work reported in this paper.

Acknowledgments

This work was supported by JSPS KAKENHI grant numbers 16H04601 and 19H02362. The authors would like to thank T. Imamoto and K. Fujiwara for technical assistance with the experiments.

References

[1] Henham A, Makkar MK. Combustion of simulated biogas in a dual-fuel diesel engine. Energy Convers Manage 1998;39(16-18):2001–9.
[2] Barik D, Murugan S. Investigation on combustion performance and emission characteristics of a DI (direct injection) diesel engine fueled with biogas–diesel in dual fuel mode. Energy 2014;72:760–71.
[3] Kim Y, Kawahara N, Tsuboi K, Tomita E. Combustion characteristics and NO_X emissions of biogas fuels with various CO_2 contents in a micro co-generation spark-ignition engine. Appl Energy 2016;182:539–47.
[4] Tippayawong N, Promwungkwa A, Rerkkriangkrai P. Long-term operation of a small biogas/diesel dual-fuel engine for on-farm electricity generation. Biosyst Eng 2007;98(1):26–32.
[5] Huang J, Crookes RJ. Assessment of simulated biogas as a fuel for the spark ignition engine. Fuel 1998;77(15):1793–801.
[6] Bade Shrestha SO, Narayanan G. Landfill gas with hydrogen addition – A fuel for SI engines. Fuel 2008;87(17-18):3616–26.
[7] Porpatham E, Ramesh A, Nagalingam B. Investigation on the effect of concentration of methane in biogas when used as a fuel for a spark ignition engine. Fuel 2008;87(8-9):1651–9.
[8] Verma S, Das LM, Kaushik SC. Effects of varying composition of biogas on performance and emission characteristics of compression ignition engine using exergy analysis. Energy Convers Manage 2017;138:346–59.
[9] Aklouche FZ, Loubar K, Bentebbiche A, Awad S, Tazerout M. Experimental investigation of the equivalence ratio influence on combustion, performance and exhaust emissions of a dual fuel diesel engine operating on synthetic biogas fuel. Energy Convers Manage 2017;152:291–9.
[10] Barik D, Satapathy AK, Murugan S. Combustion analysis of the diesel–biogas dual fuel direct injection diesel engine – the gas diesel engine. Int J Ambient Energy 2017;38(3):259–66.
[11] Bora BJ, Saha UK. Optimization of injection timing and compression ratio of a raw biogas powered dual fuel diesel engine. Appl Therm Eng 2016;92:111–21.
[12] Bora BJ, Saha UK, Chatterjee S, Veer V. Effect of compression ratio on performance, combustion and emission characteristics of a dual fuel diesel engine run on raw biogas. Energy Convers Manage 2014;87:1000–9.
[13] Makareviciene V, Sendzikiene E, Pukalskas S, Rimkus A, Vegneris R. Performance and emission characteristics of biogas used in diesel engine operation. Energy Convers Manage 2013;75:224–33.
[14] Ambarita H. Performance and emission characteristics of a small diesel engine run in dual-fuel (diesel-biogas) mode. Case Studies Thermal Eng 2017;10:179–91.
[15] Feroskhan M, Ismail S. Investigation of the effects of biogas composition on the performance of a biogas–diesel dual fuel CI engine. Biofuels 2016;7(6):593–601.
[16] Cacua K, Amell A, Cadavid F. Effects of oxygen enriched air on the operation and performance of a diesel-biogas dual fuel engine. Biomass Bioenergy 2012;45:159–67.
[17] Kalsi SS, Subramanian KA. Effect of simulated biogas on performance, combustion and emissions characteristics of a bio-diesel fueled diesel engine. Renewable Energy 2017;106:78–90.
[18] Yoon SH, Lee CS. Experimental investigation on the combustion and exhaust emission characteristics of biogas–biodiesel dual-fuel combustion in a CI engine. Fuel Process Technol 2011;92(5):992–1000.
[19] Sahoo BB, Sahoo N, Saha UK. Effect of engine parameters and type of gaseous fuel on the performance of dual-fuel gas diesel engines—A critical review. Renew Sustain Energy Rev 2009;13(6-7):1151–84.
[20] Park SH, Yoon SH, Cha J, Lee CS. Mixing effects of biogas and dimethyl ether (DME) on combustion and emission characteristics of DME fueled high-speed diesel engine. Energy 2014;66:413–22.
[21] Barik D, Murugan S, Sivaram NM, Baburaj E, Shanmuga Sundaram P. Experimental investigation on the behavior of a direct injection diesel engine fueled with Karanja methyl ester-biogas dual fuel at different injection timings. Energy 2017;118:127–38.
[22] Bora BJ, Saha UK. Experimental evaluation of a rice bran biodiesel – biogas run dual fuel diesel engine at varying compression ratios. Renewable Energy 2016;87:782–90.
[23] Karim GA. An examination of some measures for improving the performance of gas fuelled diesel engines at light load. SAE Paper No.912366 1991.
[24] Wang Z, Zhao Z, Wang D, Tan M, Han Y, Liu Z, Dou H. Impact of pilot diesel ignition mode on combustion and emissions characteristics of a diesel/natural gas dual fuel heavy-duty engine. Fuel 2016;167:248–56.
[25] Bedoya ID, Saxena S, Cadavid FJ, Dibble RW, Wissink M. Experimental study of biogas combustion in an HCCI engine for power generation with high indicated efficiency and ultra-low NOx emissions. Energy Convers Manage 2012;53(1):154–62.
[26] Swami Nathan S, Mallikarjuna JM, Ramesh A. An experimental study of the biogas–diesel HCCI mode of engine operation. Energy Convers Manage 2010;51(7):1347–53.
[27] Bedoya ID, Saxena S, Cadavid FJ, Dibble RW, Wissink M. Experimental evaluation of strategies to increase the operating range of a biogas-fueled HCCI engine for power generation. Appl Energy 2012;97:618–29.
[28] Park SH, Yoon SH. Effect of dual-fuel combustion strategies on combustion and emission characteristics in reactivity controlled compression ignition (RCCI) engine. Fuel 2016;181:310–8.
[29] Bates L, Bradley D, Gorbatenko I, Tomlin AS. Computation of methane/air ignition delay and excitation times, using comprehensive and reduced chemical mechanisms and their relevance in engine autoignition. Combust Flame 2017;185:105–16.
[30] Kawahara N, Tomita E, Sakata Y. Auto-ignited kernels during knocking combustion in a spark-ignition engine. Proc Combust Inst 2007;31(2):2999–3006.
[31] Bates L, Bradley D, Paczko G, Peters N. Engine hot spots: Modes of auto-ignition and reaction propagation. Combust Flame 2016;166:80–5.
[32] Azimov U, Tomita E, Kawahara N, Harada Y. Premixed mixture ignition in the end-gas region (PREMIER) combustion in a natural gas dual-fuel engine: operating range and exhaust emissions. Int J Engine Res 2011;12(5):484–97.
[33] Azimov U, Tomita E, Kawahara N, Harada Y. Effect of syngas composition on combustion and exhaust emission characteristics in a pilot-ignited dual-fuel engine operated in PREMIER combustion mode. Int J Hydrogen Energy 2011;36(18):11985–96.
[34] Aksu C, Kawahara N, Tsuboi K, Kondo M, Tomita E. Extension of PREMIER combustion operation range using split micro pilot fuel injection in a dual fuel natural gas compression ignition engine: A performance-based and visual investigation. Fuel 2016;185:243–53.
[35] Kawahara N, Kim Y, Wadahama H, Tsuboi K, Tomita E. Differences between PREMIER combustion in a natural gas spark-ignition engine and knocking with pressure oscillations. Proc Combust Inst 2019;37(4):4983–91.
[36] Valipour Berenjestanaki A, Kawahara N, Tsuboi K, Tomita E. End-gas autoignition characteristics of PREMIER combustion in a pilot fuel-ignited dual-fuel biogas engine. Fuel 2019;254:115634. https://doi.org/10.1016/j.fuel.2019.115634.
[37] Tingas EA, Im HG, Kyritsis DC, Goussis DA. The use of CO_2 as an additive for ignition delay and pollutant control in CH_4/air autoignition. Fuel 2018;211:898–905.